Modelling of complex boron dilution transients in PWRs—Validation of CFD simulation with ANSYS CFX against the ROCOM E2.3 experiment

Grahn, A.; Diaz Pescador, E.; Kliem, S.; Schäfer, F.; Höhne, T.;

Originally published:

February 2021

Nuclear Engineering and Design 372(2021), 110938

DOI: https://doi.org/10.1016/j.nucengdes.2020.110938

Perma-Link to Publication Repository of HZDR:

https://www.hzdr.de/publications/Publ-30093

Advanced modelling of complex boron dilution transients in PWRs — Part II: Validation of CFD simulation with ANSYS CFX against ROCOM E2.3 experiment

A. Grahn[a], E. Diaz Pescador[a,b], S. Kliem[a,*], F. Schäfer[a], T. Höhne[a]

[a] *Helmholtz-Zentrum Dresden-Rossendorf, Dresden, Germany*
[b] *Technische Universität Dresden, Dresden, Germany*

Abstract

This part of a series of two papers compares CFD simulation results of a boron dilution scenario with experimental results. The simulation was carried out with ANSYS CFX using the SST turbulence scheme, experimental data were produced in the ROCOM test facility, experiment E2.3. The main features of the scenario are asymmetric, transient mass flow conditions in the affected loops 1 and 2 of a KONVOI-type reactor vessel and reduced density of the underborated coolant slugs fed into the reactor trough the cold legs of both loops. The CFD simulation was able to capture the density stratification in the loops affected by underboration and the mixing in the downcomer and in the lower plenum. Good agreement with the experiment was obtained for the temporal evolution of average boron concentration in several measuring sections of the reactor vessel and of the boron distribution in the core inlet. In general, minimal values of boron concentration were found to be lower in the simulation than in the experiment.

Keywords: Boron dilution, ROCOM, ANSYS CFX, Validation

1. Introduction

Boron is a neutron absorber. In pressurized water reactors, it is added as boric acid to the primary loop coolant at varying concentrations over the fuel cycle in order to remove excess reactivity from the reactor core. Under normal conditions with forced circulation, boric acid is homogeneously dissolved in the coolant inventory. In the aftermath of a small break loss of coolant accident (SB LOCA), decay heat is removed from the core by coolant evaporation. Subsequent condensation in the steam generator leads to the formation of underborated liquid coolant that accumulates in the loop seals of the primary circuit. After refilling and restart of natural circulation, slugs of underborated coolant reach the reactor core and give rise to re-criticality and power insertion.

*Corresponding author
Email address: mailto:s.kliem@hzdr.de (S. Kliem)

Hyvärinen (1993) identifies this scenario as inherent boron dilution because it results from separating the regular coolant inventory into boron-rich and boron-free portions. Another source of underboration that may happen under normal operation is inadvertent injection of boron-free coolant from external sources, such as the accumulator.

Boron dilution was identified as a key issue of PWR safety. Its analysis is part of the design and of the licensing and oversight procedures. A recommendation issued by the German Reactor Safety Commission (RSK) defines a minimal target value of boron concentration that ensures subcriticality during shut-down and transient events (RSK, 2012). Boron dilution has been the subject of experimental studies in medium and large scale test facilities as well as their numerical analysis (Alvarez et al., 1992; Bucalossi et al., 2011; Hertlein et al., 2003; Kliem et al., 2008a,b, 2007; Umminger et al., 2001, 2002; Woods et al., 2000). These studies have shown that coolant mixing in the cold legs, downcomer and lower plenum may not always re-establish the required boron concentration over the whole core cross section.

Single phase natural circulation flow with liquid mixing is still a challenging task for numerical analysis. There are two main categories of simulation tools currently used in reactor safety analysis, thermal-hydraulic system codes, such as ATHLET, CATHARE and TRACE, and computational fluid dynamic codes, such as OpenFOAM, ANSYS CFX and STAR-CCM+. Current developments have added coarse-mesh 3D modelling capabilities to system codes in order to capture more complex flow phenomena including coolant mixing in large geometries. A recently published study compares system and CFD codes that simulated flow mixing after cold leg accumulator injection (Bousbia Salah et al., 2018). Kliem et al. (2010) performed a boron dilution experiment in the ROCOM test facility and subsequent CFD simulation. Based on an SB LOCA scenario, it used symmetric boundary conditions of concentration and mass flow rates at the core inlets as well as uniform density.

The present Part II of a series of two papers compares simulation results obtained with the CFD code ANSYS CFX against the ROCOM E2.3 experiment (Kliem and Sühnel, 2006) and against the simulation results obtained with the system code ATHLET 3.1A, presented in detail in Part I (Pescador et al., 20??). Experiment E2.3 is focussed on fluid mixing in the cold legs and in the reactor vessel during a boron dilution event. Contrary to (Kliem et al., 2010), it postulates asymmetric inlet coolant mass flow rates and different densities of the underborated slugs and the coolant inventory.

2. ROCOM test facility and experiment

The ROCOM (ROssendorf COolant Mixing) test facility (Kliem et al., 2008a) was a 1:5 mock-up of the German four-loop pressurized water reactor KONVOI (Siemens KWU) including the primary coolant circuit. Made of acrylic glass, the vessel includes components interacting with the velocity field such as the core barrel with the lower core support plate, the perforated drum and core channels. Now dismantled, it was located at Helmholtz-Zentrum Dresden-Rossendorf (HZDR) in Germany and was designed for the investigation of a wide spectrum of fluid mixing scenarios (Prasser et al., 2003).

The facility was mainly filled with de-ionized water at room temperature and operated at atmospheric pressure. It is instrumented with so-called wire-mesh

sensors which are two-dimensional arrays of conductivity probes. They allow the mixing of coolant portions, in parts labelled with kitchen salt as a tracer, to be recorded in real-time. Wire-mesh sensors are installed at cross sections of the cold-side loop conducts, across the annular gap at the top and low ends of the downcomer, on the downcomer walls, and in the inlet openings of the 193 core tubes.

The ROCOM E2.3 experiment, serving as the validation base for the present CFD study, is described in Part I of this series of papers (Pescador et al., 20??). In essence, ROCOM E2.3 emulates a boron dilution transient after onset of natural convection in the late phase of a small-break LOCA in the hot side of the primary circuit. Unlike previous experiments, E2.3 considers *asymmetric* flow conditions with underborated slugs arriving at different and time-dependent mass flow rates trough two neighbouring vessel inlets (loops 1 and 2), while the other loops 3 and 4 remain unaffected from underboration and mass flow changes.

3. Numerical modelling with ANSYS CFX

ANSYS CFX is a general-purpose fluid dynamics simulation software which has been applied across a wide range of CFD and multi-physics applications. Phenomena that can be simulated and that are relevant for conventional and nuclear power generation applications include turbulent multiphase flow, heat and mass transfer, and flow in rotating geometries such as pumps, fans, compressors and turbines.

ANSYS CFX solves the Navier-Stokes equations using an element-based finite-volume method with second-order discretization schemes in space and time. It works on structured and unstructured types of grids as well as on mixtures of both that allow different mesh cell geometries, such as hexahedra, tetrahedra and prisms, to be aligned in any arrangement. A coupled algebraic multigrid algorithm results in high convergence rates and the solver can be run in parallel on computing clusters in order to deal with large problem cases.

3.1. Numerical model

Any numerical method is inseparably associated with numerical and model errors. The former arise from discretising the governing, differential equations into large sets of algebraic equations based on numerical grids of given granularity and on finite time step sizes, the latter from neglecting certain physical phenomena, their approximation with empirical equations and from other simplifications. Spatial and temporal refinement of the solution are limited by hardware and calculation time restrictions, while the adequate description of the physical process depend on the current knowledge and the availability of mathematical models. For CFD applications in reactor safety analysis Best Practice Guidlines (BPG) have been developped in order to quantify remaining errors and to find an acceptable trade-off between accuracy and simulation costs (Mahaffy et al., 2014). The computational mesh of the present study was built and the numerical models were selected in compliance with these guidelines. Corresponding investigatons have been carried out in (Höhne et al., 2008; Kliem et al., 2010; Rohde et al., 2007).

The computational domain is shaped after the ROCOM test facility and is shown in Fig. 1. It entails the reactor vessel mock-up with loop inlet nozzles,

Table 1: Coolant and slug properties

Fluid	Temperature (°C)	Density ($\mathrm{kg\,m^{-3}}$)	Viscosity (mPa s)
Coolant	20	998.158	1.002 14
Slug	20	995.722	1.050 42

downcomer, lower plenum with perforated drum, core support and reactor core, but only the upstream parts of the coolant loops which are relevant for the investigated mixing scenario. All vessel built-ins are reproduced in detail, such as the lower plenum shown in Fig. 2 and the core region consisting of 193 tubes. As in the actual ROCOM E2.3 experiment, the cold-leg sections of loops 1 and 2, which are highlighted in Fig. 1, hold the entire volume of underborated coolant at the start of transient calculation.

The numerical grid of the ROCOM vessel was developed for a previous mixing study (Kliem et al., 2010). Based on a meshing study a spatial resolution of 4.2 million cells was selected, where the lower plenum, due to its complex geometry, is completely filled with tetrahedra, the remaining parts with hexahedral cells.

For modelling turbulence the CFX-builtin Shear Stress Transport (SST) model with automatic wall function and buoyancy induced turbulence, option "Production and Dissipation" were selected. The SST model solves a turbulence/frequency-based model (k–ω) at the wall and the turbulence kinetic energy/dissipation model (k–ε) in the bulk flow. The High-Resolution scheme was used for discretizing the convective and diffusive transport terms, the second order Backward-Euler scheme with adaptive time step size for temporal discretization. The initial time step size of the transient simulation was 0.001 s.

3.2. Boundary conditions

The ROCOM experiment was conducted at room temperature (20 °C) and ambient pressure (1 bar). The same, isothermal conditions were imposed on the simulation. The physical properties of the coolant and of the underborated slug correspond to the experimental conditions. As in the ROCOM experiment, pure water represents the coolant with nominal boron concentration, and a water-ethanol mixture with a density ratio of 0.997 56 with respect to pure water represents the underborated slug. In the experiment, a small amount of kitchen salt was added to the slug mixture, serving as a tracer for the conductivity-based concentration measurement. In the simulation it was neglected as it does not change the viscosity of the slug. Coolant and slug properties are summarized in Table 1.

At the inlet boundaries of loops 1 to 4, denoted by inward directed arrows in Fig. 1, time-dependent coolant mass flow rates as in the ROCOM experiment are imposed. They are plotted in Fig. 3. Contrary to a previous study (Kliem et al., 2010) with monotonically increasing and identical mass flows in all four loops, mass flows in loops 1 and 2 are characterized here by strong perturbations. As in the ROCOM experiment, time zero is shifted to the start of natural convection-driven coolant circulation in loops 1 and 2. The coolant fed into the domain during the transient is of nominal boron concentration. It displaces

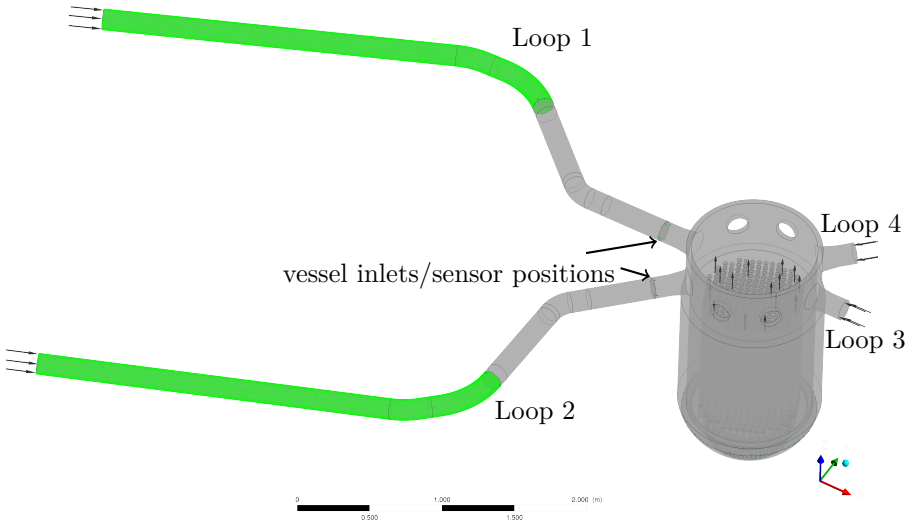

Figure 1: Computational domain with highlighted loop sections initially filled with underborated coolant

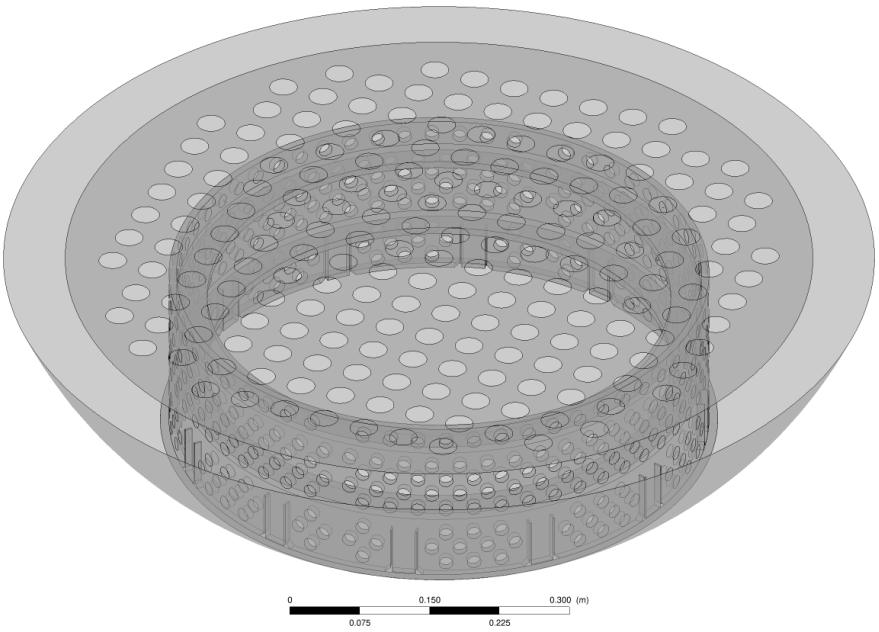

Figure 2: Lower plenum and core support of the CFD model

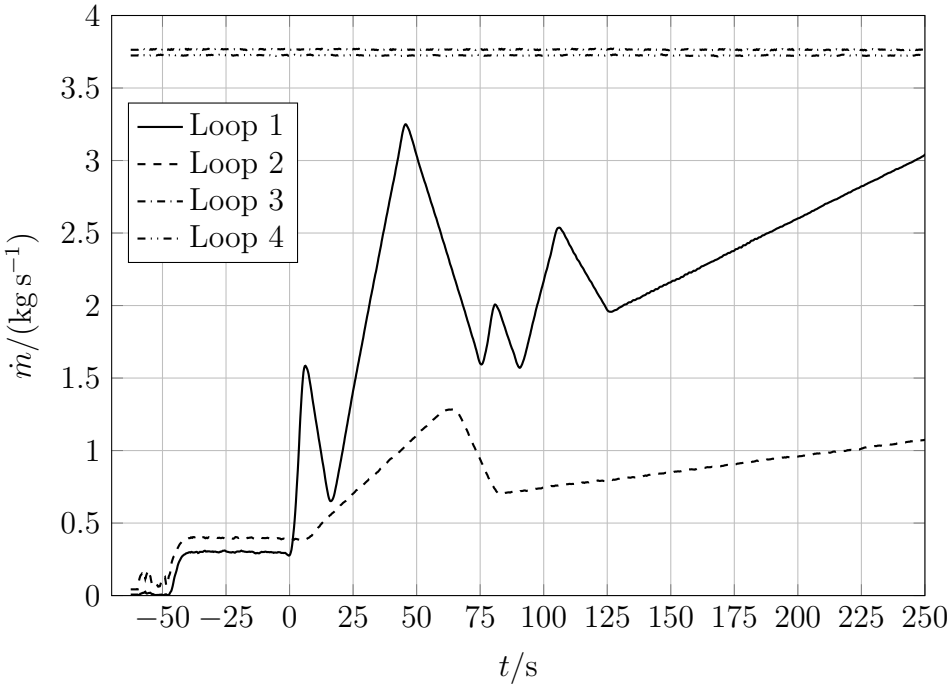

Figure 3: Coolant mass flows at inlet boundaries

the underborated slugs in loops 1 and 2 from their initial positions (highlighted sections), pushing them towards the reactor vessel. Both slugs have an initial volume of 57.6 litres. The upper openings of the 193 core tubes constitute the outlet boundary where constant atmospheric pressure is assigned.

Prior to starting the transient simulation, a steady state calculation was performed to obtain the initial state of the flow field to start from. In the steady state, the whole domain is filled with regular coolant, corresponding to nominal boron concentration, and identical coolant is entering through the cold legs of all four loops with mass flow rates as of $t = 62.5\,\mathrm{s}$, which is the starting point of the curves in Fig. 3.

4. Simulation results

When the transient simulation starts, the concentration fronts of the slugs are located 1.80 m upstream of the vessel inlets 1 and 2 (cf. Fig. 1). This corresponds to the starting time of the experiment, when the valves in loops 1 and 2 are opened in order to release the slugs from their initial positions. While loops 3 and 4 are operated at constant mass flow rates of about $3.7\,\mathrm{kg\,s^{-1}}$ throughout the simulation, loops 1 and 2 are kept at low values of 0.3 and $0.4\,\mathrm{kg\,s^{-1}}$ for about 40 seconds. This first stage of the experiment was supposed to give time for the slug fronts to reach the vessel inlets at a low flow velocity before starting the pump ramps.

However, according to the concentration curves in Fig. 4, arrival of slug water at the inlet nozzle planes is detected earlier in the experiment and in

the CFX simulation. Measured and simulated boron distributions in the inlet cross sections, Fig. 5, indicate that slug and regular coolant are layered one on top of the other. After opening the valves, the initially vertical concentration front is tipping over because of the different densities of the fluids. In the top half of the pipe, the lighter, underborated slug is moving towards the vessel faster than average flow speed, while regular coolant is moving in the opposite direction on the pipe's bottom. The concentration profiles over time found by CFX agree quantitatively well with the experimental profiles. After 70 s, the slug inventory from loop 1 has been completely injected into the reactor vessel in both experiment and CFX simulation. On the other hand, due to the lower mass flow rate this takes much longer to accomplish in loop 2, that is, 210 s in the CFX simulation and about 250 s in the experiment. Despite this discrepancy, agreement between CFX and the experiment is still good, as the simulation curve follows closely the experimental one over a large time span. The plotted time dependencies suggest that three-dimensional CFD is able to properly simulate buoyancy-driven fluid mixing in the pipe section.

ATHLET, on the other hand, solves the one-dimensional transport equations for pipe flow and thus cannot reproduce the density stratification of the coolant. Hence, the slugs arrive at the inlet nozzles around the planned starting time of the pumps, fairly on time at $t = 0$ s in the case of loop 1 and somewhat earlier in loop 2 because of the slightly higher initial mass flow rate. Ideally, a one-dimensional solution should produce a step-like time dependency of concentration, but numerical diffusion leads to a dispersion of the concentration front along the pipe axis and hence the shape of the ATHLET curves in Fig. 4.

Coolant mixing in the downcomer region is qualitatively assessed in Fig. 6. It shows boron distributions in the unwrapped downcomer at different times obtained in the experiment and in the CFX simulation. The displayed values correspond to the average value across the width of the downcomer gap. Loop 1 and 2 inlet positions are at 157.5° and 202.5°. At the beginning, when mass flow rates of loops 1 and 2 are small as compared to loops 3 and 4, the underborated coolant slugs tend to merge half-way between the azimuthal inlet positions of loop 1 and 2, forming a single plume with the minimal boron concentration at $\varphi = 180°$. Later on, with higher flow rates in loops 1 and 2, the predominance of loops 3 and 4 diminishes, allowing the formation of two distinct boron minima about the downcomer circumference. Both simulated and experimental distributions resemble each other, presenting similar vortex-like flow structures. However, the boron distribution appears to be more diffusive in the experiment.

Fig. 7 plots the time dependency of boron concentration that was measured in three horizontal planes located at the top, at the half height and at the bottom of the downcomer. For the plots in the left column, concentration was averaged over the wire-mesh node values, and the minimal values found were used for the right column. The timings of the curve minima are similar between experiment, CFX and ATHLET with differences below 15 s. From the top down to the bottom measuring planes, the agreement of the average concentration curves improves for ROCOM and the CFX simulation. In the top plane, CFX underestimates the experimental value by about 250 ppm and by about 50 ppm in the bottom plane. For the minimal concentration curves it is the opposite, were CFX increasingly underestimates the experimental concentration. For ATHLET, one observes a faster passage of the underborated coolant slug through the measuring planes, with steep gradients in the falling and rising slopes. Also,

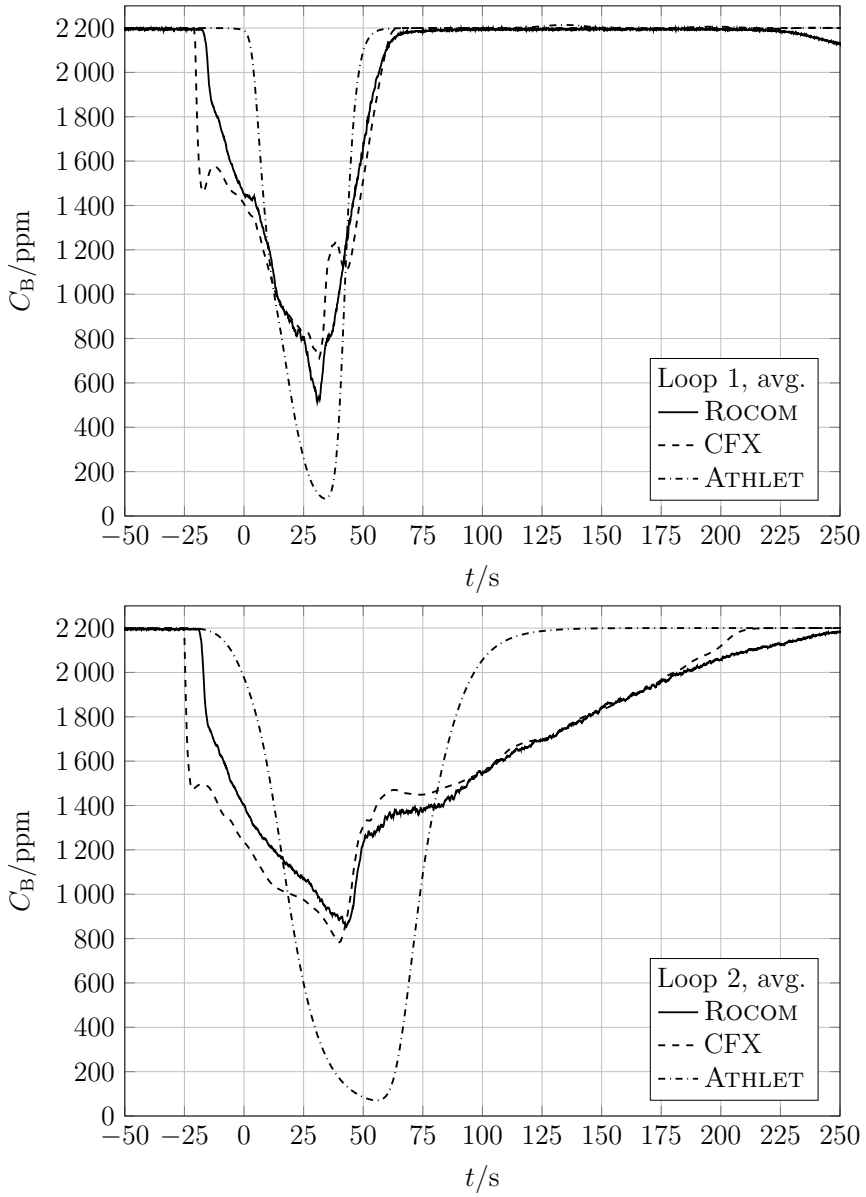

Figure 4: Boron concentration at vessel inlets of loops 1 and 2; arithmetic average over values at wire-mesh nodes (experiment and CFX), single-valued result of ATHLET

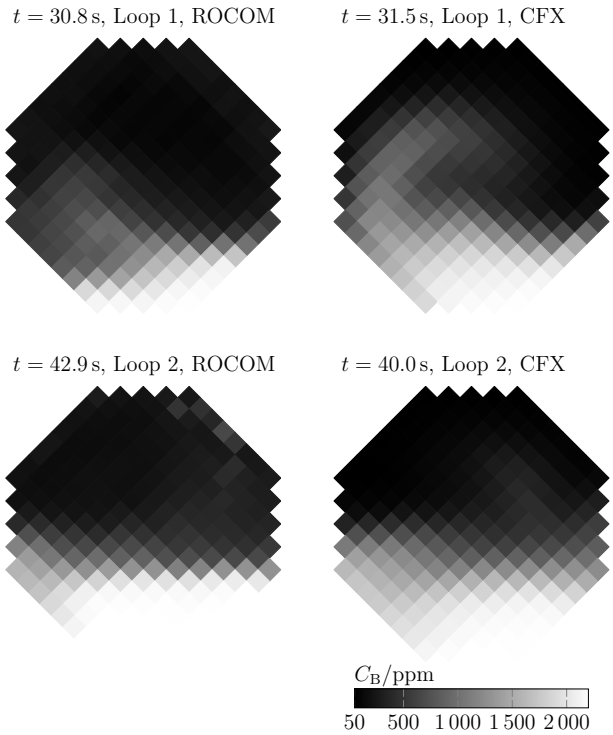

Figure 5: Boron distribution at inlet sensor positions of loops 1 and 2 at time of minimal area-averaged concentration; left: experiment, right: CFX

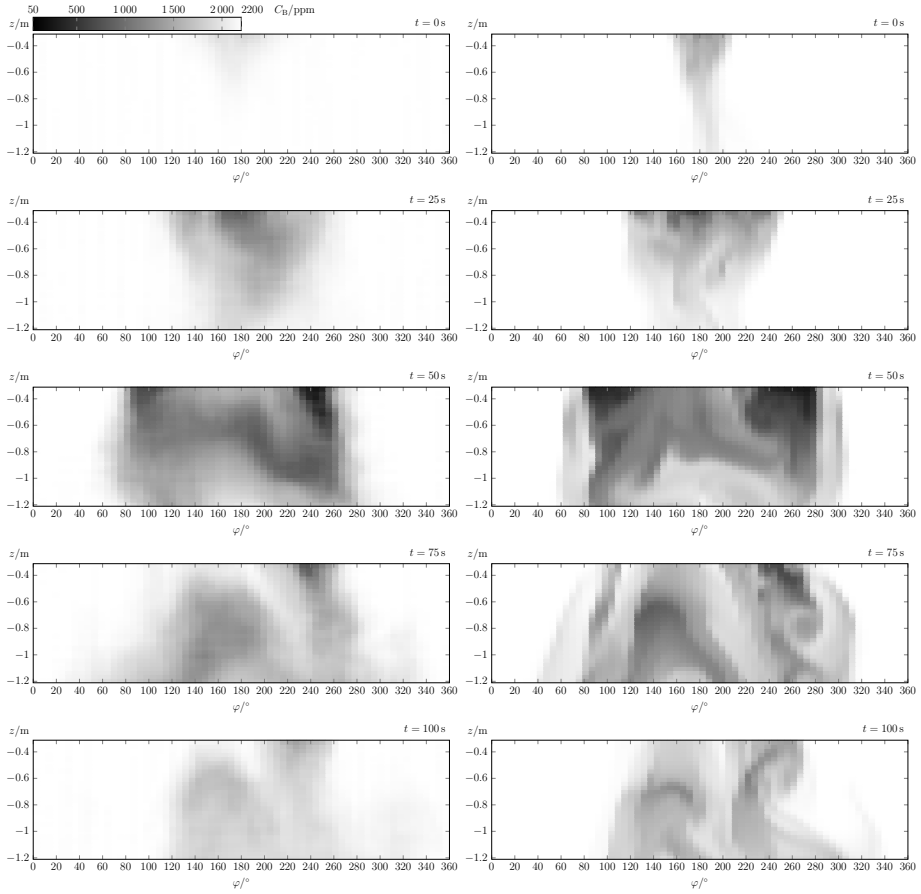

Figure 6: Boron distribution in the unwrapped downcommer at different times; left: experiment, right: CFX

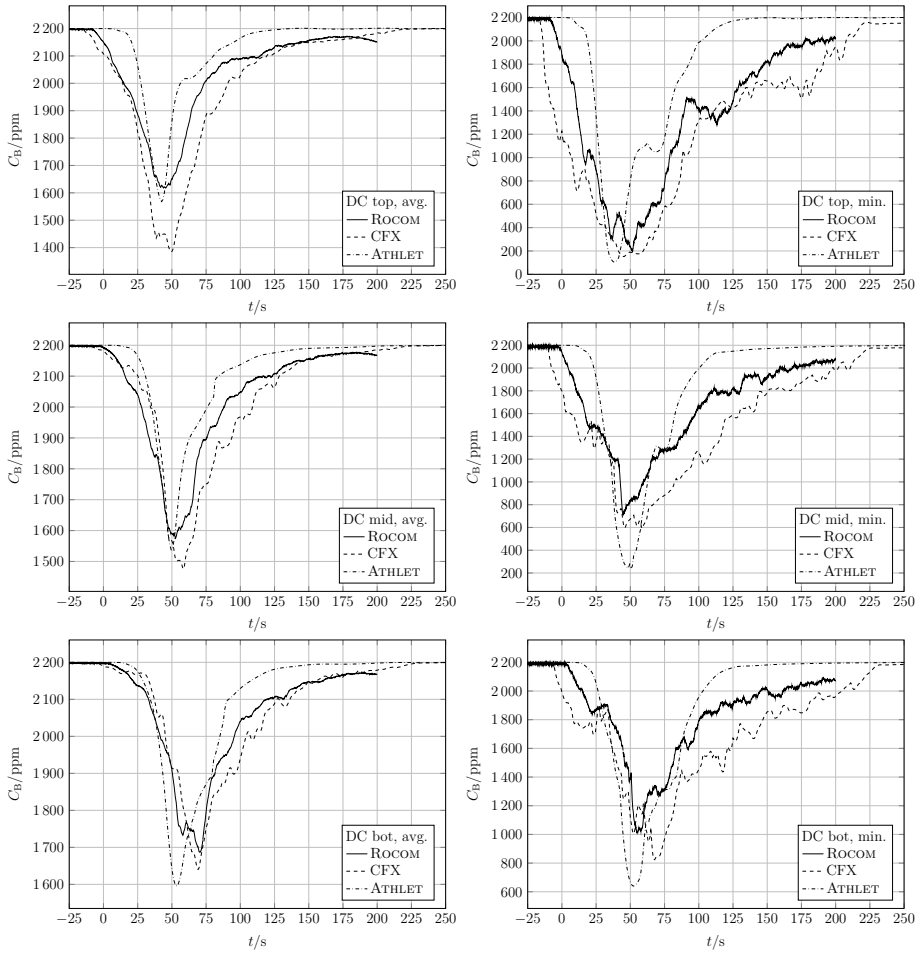

Figure 7: Average (left) and minimal boron concentration (right) in horizontal downcomer top, mid and bottom cross sections

ATHLET underestimates the boron concentration around the curve minima.

The time dependencies of average and minimal boron concentration in the entire downcomer region are shown in Fig. 8. The plots also contain the P2 confidence range of the measured values which was obtained from repeated realisations of the experiment(Kliem et al., 2008b). For the simulations, timings of the curve minimum are in good agreement with the experiment. Curves from simulations fall only partly within the confidence range of the experiment, and the CFX simulation tends to underestimate the measured values in general.

Fig. 9 compares measured and calculated time curves of boron concentration at three monitor points in the downcomer. The locations were selected to lie on a vertical line between the azimuthal positions of loops 1 and 2. This part of the downcomer is strongly affected by mixing of the coolant streams stemming from these loops, as shown by the time series in Fig. 6. At the top position and at the half height of the downcomer the minimum passes around the same time in the experiment and the simulation and so do the absolute minimal concentrations. The simulation curves differ in two aspects from the experiment. First, concen-

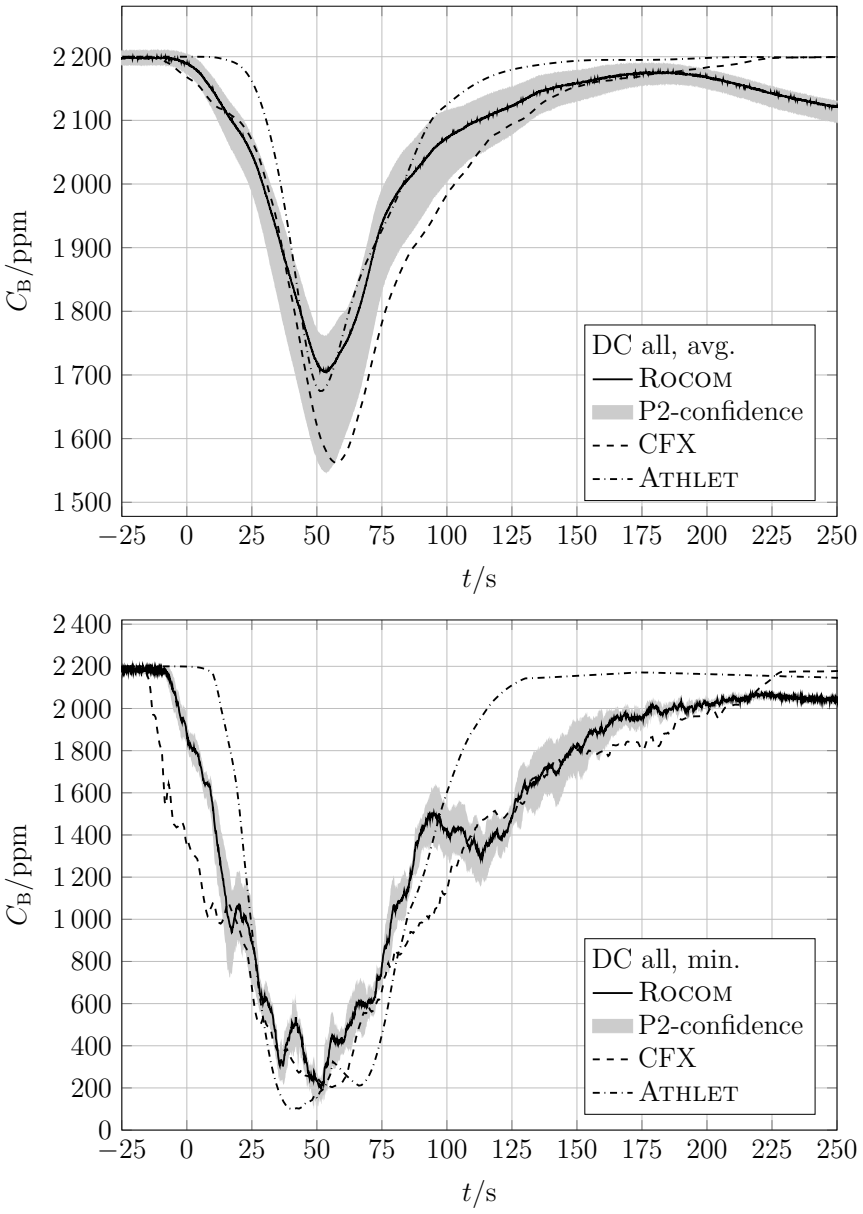

Figure 8: Average and minimal boron concentration in the whole downcomer region

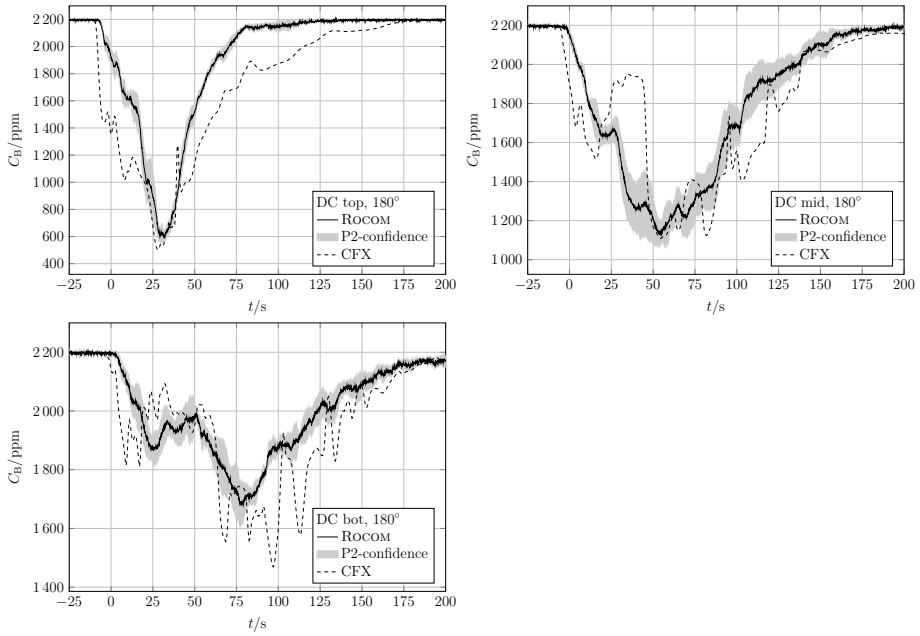

Figure 9: Boron concentration at three points along the vertical line at $\varphi = 180°$ in the downcomer

tration drops faster at the beginning and second, stronger fluctuations develop while the slug travels downward. This is an indication of a higher mixing rate in the experiment in contrast to sharper concentration gradients that establish during the simulation. It is also supported by the more diffusive boron distribution in the experiment, as can be seen in Fig. 6. At the bottom position, the minimal value of the simulated boron concentration lags behind the minimum passage in the experiment by about 20 s. The underborated slug is lighter than the surrounding coolant which opposes its downward movement through the downcomer. This effect is stronger in the simulation were mixing is less intense than in the experiment, finally leading to the observed lag. Moreover, since concentration is monitored at a fixed spot of the vessel, a small displacement of the slug plume between experiment and simulation may significantly influence the time dependency of the recorded values.

In the core inlet plane (Fig. 10), the calculated average boron concentration agrees well with the experimental result, with large parts of the curve lying within the P2 confidence. Nevertheless, the CFX simulation underestimates the minimal concentration and the global minimum lags behind the experiment by about 12 s. Two-dimensional boron distributions are shown in Fig. 11. The time of the snapshot was chosen at the global minimum in the simulation. In both experiment and CFX simulation, this is around the minimal value of the average boron concentration in the core inlet plane (cf. upper picture in Fig. 10). Both distributions are very similar: underboration dominates the peripheral coolant channels, with the exception of those which are close to the inlet positions of loops 3 and 4. Furthermore, there is a band of underboration across the central part creating two zones of channels with little underboration.

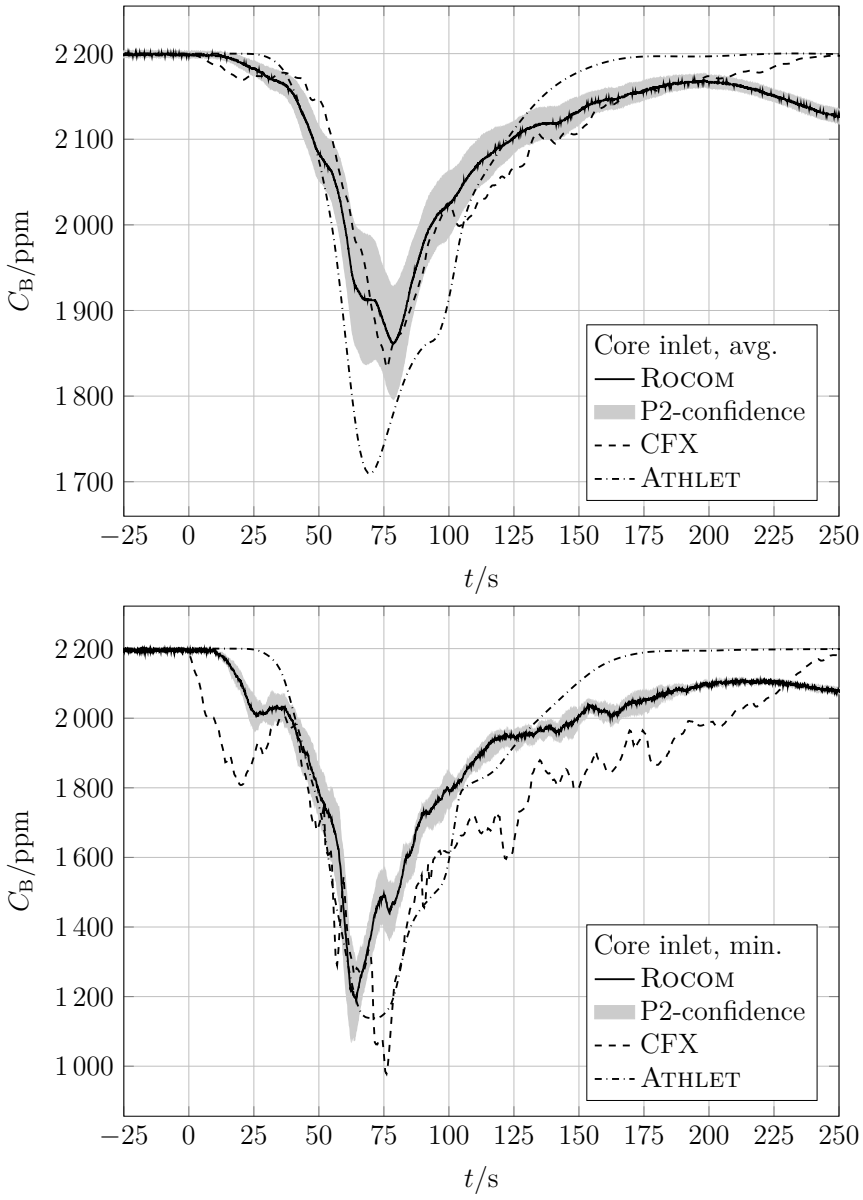

Figure 10: Average and minimal boron concentration in the core inlet plane

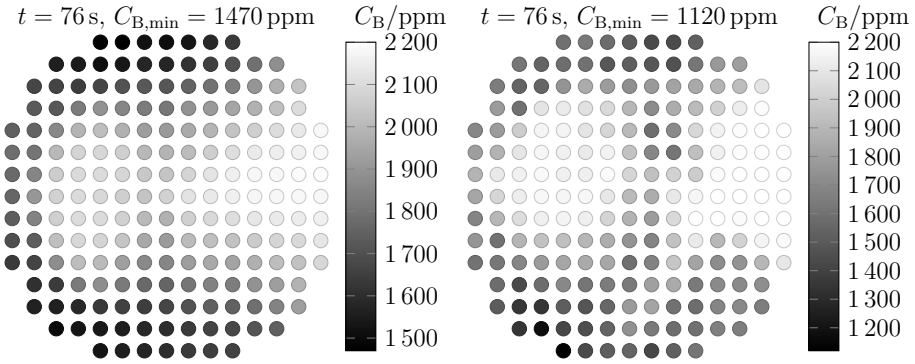

Figure 11: Boron distribution in the core inlet; snapshot around time of minimal average concentration; left: experiment, right: CFX

5. Conclusions

This paper reports on a validation study of the 3D CFD code ANSYS CFX against the boron dilution experiment E2.3 carried out at the ROCOM facility. The experiment features asymmetry in the coolant mass flows in the cold legs of loops 1 and 2, simulating the restart of natural circulation, as well as slugs of underborated coolant at lower density than the normal coolant which enter the reactor vessel through both loops.

The CFD simulation, which uses the SST model to close the Reynolds-averaged Navier–Stokes equations, captures the main flow features qualitatively well. In particular, the stratification of the underborated slugs and of the regular coolant in the loop nozzles of the reactor vessel could be reproduced with good agreement. Similar vortex structures and shapes of the slug plumes propagating through the downcomer were observed in the simulation and in the experiment. The temporal evolution of averaged simulated boron concentration follows closely the experimental curves in most measuring planes. In the core inlet plane, regions of lower and higher boron concentration are similarly distributed in the simulation and in the experiment.

Perturbations of the mass flow rates in loops 1 and 2, which are imposed by the experimental conditions, give rise to vortex flow structures and erratic movement of the underborated coolant plumes on their way through the downcomer and the lower plenum. Therefore, the local boron concentration recorded at several monitoring points in the downcomer and also the minimal concentration in the core inlet display noticeable oscillations, which are stronger in the CFD simulation than in the experiment. This and the generally lower calculated minimal values suggest that the simulation underestimates the rate of coolant mixing. Future CFD studies will focus on resolving this discrepancy.

Acknowledgement

The calculations using the system code ATHLET were funded by the German Federal Ministry for Economic Affairs and Energy (BMWi) with the grant number 1501540 on the basis of a decision by the German Bundestag.

References

D. Alvarez et al. Three-dimensional calculations and experimental investigations of the primary coolantflow in a 900 MW PWR vessel. In *NURETH 5 Proceedings*, pages 586–589, Salt Lake City, USA, 1992.

ANSYS CFX. URL: https://www.ansys.com/products/fluids/ansys-cfx. [Online; accessed: 2019-12-01].

A. Bousbia Salah et al. Unsteady single-phase natural-circulation flow mixing prediction using 3-D thermal-hydraulic system and CFD codes. *Nuclear Technology*, 203(3):293–314, 2018.

A. Bucalossi, F. Moretti, D. Melideo, A. Del Nevo, F. D'Auria, T. Höhne, E. Lisenkov, and D. Gallori. Experimental investigation of in-vessel mixing phenomena in a VVER-1000 scaled test facility during unsteady asymmetric transients. *Nuclear Engineering and Design*, 241(8):3068–3075, 2011.

R. J. Hertlein et al. Experimental and Numerical Investigation of Boron Dilution Transients in Pressurized Water Reactors. *Nuclear Technology*, 141(1):88–107, 2003.

J. Hyvärinen. The inherent boron dilution mechanism in pressurized water reactors. *Nuclear Engineering and Design*, 145(1):227–240, 1993.

T. Höhne, S. Kliem, U. Rohde, and F.-P. Weiss. Boron dilution transients during natural circulation flow in PWR — experiments and CFD simulations. *Nucl. Eng. Design*, 238:1987–1995, 2008.

S. Kliem and T. Sühnel. Experimente and der Versuchsanlage ROCOM zur Bestimmung der minimalen Borkonzentration bei postulierten Störfällen mit kleinem Leck im heißen Strang. Technical Report FZD/FWS/2006/03, Forschungszentrum Dresden-Rossendorf, 2006.

S. Kliem, H.-M. Prasser, T. Sühnel, F.-P. Weiss, and A. Hansen. Experimental determination of the boron concentration distribution in the primary circuit of a PWR after a postulated cold leg small break loss-of-coolant-accident with cold leg safety injection. *Nuclear Engineering and Design*, 238:1788–1801, 2008a.

S. Kliem, T. Sühnel, U. Rohde, T. Höhne, H.-M. Prasser, and F.-P. Weiss. Experiments at the mixing test facility ROCOM for benchmarking of CFD codes. *Nuclear Engineering and Design*, 238:566—-576, 2008b.

S. Kliem, T. Höhne, U. Rohde, and F.-P. Weiss. Experiments on slug mixing under natural circulation conditions at the ROCOM test facility using high resolution measurement technique and numerical modeling. *Nucl. Eng. Design*, 240:2271–2280, 2010.

S. Kliem et al. Comparative Evaluation of Coolant Mixing Experiments at the ROCOM, Vattenfall, and Gidropress Test Facilities. *Science and Technology of Nuclear Installations*, 2007:Article ID 25950, 2007.

J. Mahaffy et al. Best Practice Guidelines for the use of CFD in Nuclear Reactor Safety Applications. Technical Report NEA/CSNI/R(2014)11, OECD-NEA, 2014.

E. Diaz Pescador, A. Grahn, S. Kliem, F. Schäfer, and T. Höhne. Advanced modelling of complex boron dilution transients in PWRs — Part I: Validation of ATHLET 3D-Module against the experiment ROCOM E2.3. *Nuclear Engineering and Design*, 20?? Submitted to journal.

H.-M. Prasser, G. Grunwald, T. Höhne, S. Kliem, U. Rohde, and F.-P. Weiss. Coolant Mixing in a Pressurized Water Reactor: Deboration Transients, Steam-Line Breaks, and Emergency Core Cooling Injection. *Nuclear Technology*, 143(1):37–56, 2003.

U. Rohde, T. Höhne, S. Kliem, B. Hemström, et al. Fluid mixing and flow distribution in the reactor circuit — Computational fluid dynamics code validation. *Nucl. Eng. Design*, 237:1639–1655, 2007.

RSK. Recommendations on the maximum allow-able critical boron concentration to ensure the sub-criticality during SB-LOCA and reflux-condenser-operation. Technical report, Reaktorsicherheitskommission (RSK), 2012.

K. Umminger et al. Thermal hydraulics of PWRS with respect to boron dilution phenomena. Experimental results from the test facilities PKL and UPTF. *Nucl. Eng. Design*, 204:191–203, 2001.

K. Umminger et al. Restart of natural circulation in a PWR — PKL test results and S-RELAP 5 calculations. *Nucl. Eng. Design*, 215:39–50, 2002.

B. Woods et al. An analysis of internal dilute slug injection in aPWR integral test facility. In *Proc. 8th Int. Conf. Nucl. Engng, ICONE-8*, Baltimore, USA, 2000.